Desalination 277 (2011) 257–264

Contents lists available at ScienceDirect

Desalination

journal homepage: www.elsevier.com/locate/desal

An analytical model for spiral wound reverse osmosis membrane modules: Part II — Experimental validation

S. Sundaramoorthy [a,*], G. Srinivasan [a,1], D.V.R. Murthy [b,2]

[a] Department of Chemical Engineering, Pondicherry Engineering College, Pondicherry, 605014, India
[b] Department of Chemical Engineering, National Institute of Technology, Karnataka, Surathkal, 575025, India

ARTICLE INFO

Article history:
Received 24 November 2010
Received in revised form 15 March 2011
Accepted 13 April 2011
Available online 8 May 2011

Keywords:
Reverse osmosis
Spiral-wound module
Analytical model
Parameter estimation
Chlorophenol

ABSTRACT

This paper presents the experimental studies carried out for validation of a new mathematical model [1] developed for predicting the performance of spiral wound RO modules. Experiments were conducted on a laboratory scale spiral wound RO module taking chlorophenol as a model solute. Experiments were carried out by varying feed flow rate, feed concentration and feed pressure and recording the readings of permeate concentration, retentate flow rate, retentate concentration and retentate pressure. A total of 73 experimental readings were recorded. The membrane transport parameters A_w (solvent transport coefficient) and B_s (solute transport coefficient) and the feed channel friction parameter b were estimated by a graphical technique developed in this work. The mass transfer coefficient k, estimated using the experimental data, was found to be strongly influenced by solvent flux and solute concentration apart from the fluid velocity. Taking the effects of solvent flux, solute concentration and fluid velocity, a new mass transfer correlation for Sherwood number is proposed in this work for the estimation of mass transfer coefficient. Comparison of model predictions with experimental observations demonstrated that the model was capable of predicting permeate concentration within 10% error, retentate rate flow within 4% error and rejection coefficient within 5% error.

1. Introduction

Although reverse osmosis (RO) got established as a successful technology for sea water desalination [2] in the early 60s, it was only in the past 20 years that RO made inroads into other applications like removal of organics and treatment of waste water [3–6]. With increasing applications of RO in the removal of organic compounds, studies on design and performance analysis of RO modules gain importance in the success of RO technology for separation of organic solutes. Spiral wound reverse osmosis membrane module [7] is widely used in industrial applications due to high packing density and lower capital and operating costs.

Development of mathematical models to predict the performance of spiral wound RO modules in removal of organic solutes is important for the optimal design and operation of these modules in such applications. Studies reported in the literature on development of mathematical models describing the performance of spiral wound RO modules include '*Approximate analytical models*' [8–13] and '*Rigorous numerical models*' [14–16]. Although numerical models are more appropriate for describing complex situations, the analytical models are useful for gaining better physical insight and understanding of the system. A new analytical model for the spiral wound RO module was developed in this study and reported in Part I of this paper series [1]. In this model [1], variations of pressure, flow and solute concentration in the feed channel of the module were incorporated and the transport through the membrane was described by solution–diffusion model with concentration polarization [17].

Validation of the mathematical model with experimental data becomes essential for the model to get accepted as an analytical tool for the design and operation of spiral wound RO modules. Most of the studies on validation of models for spiral wound RO modules were confined to sea water desalination data [13,15,18] and not many works on model validation with experiments using organic solutes were found in the literature. In this paper, experimental studies (Section 2) conducted on laboratory scale spiral wound RO module with chlorophenol as a model solute is reported. Experimental readings recorded in this work were used for validation (Section 5) of the analytical model developed and reported in Part I [1].

Parameter estimation is an important aspect of any mathematical modeling work. Model parameters are usually estimated by matching the model predictions with experimental data. Estimation of membrane transport parameters A_w (solvent transport coefficient) and B_s (solute transport coefficient) using experimental measurements on 'stirred membrane cells' is reported in the literature [19–21]. In the present

* Corresponding author. Tel.: +91 9444290056; fax: +91 413 2655101.
E-mail addresses: ssm_pec@yahoo.com (S. Sundaramoorthy), seenu_pec@yahoo.com (G. Srinivasan), dvrmvzm@gmail.com (D.V.R. Murthy).
[1] Tel.: +91 9444290056; fax: +91 413 2655101.
[2] Tel.: +91 824 2474039; fax: +91 824 2474033.

0011-9164/$ – see front matter © 2011 Elsevier B.V. All rights reserved.
doi:10.1016/j.desal.2011.04.037

Table 1
Specifications of the spiral wound membrane module.

Make	Ion exchange, India
Membrane material	TFC polyamide
Module configuration	Spiral wound
Number of turns (n)	30
Feed spacer thickness (t_f),mm	0.8
Permeate channel thickness, (t_p),mm	0.5
Membrane area(A_m), m^2	7.85
Feed channel area (A_f), m^2	6.72×10^{-3}
Permeate channel area (A_p), m^2	4.67×10^{-4}
Module length (L), m	0.934
Module diameter (D), inches	3.25
Membrane width (W), m	8.40
% salt rejection	>97%

work, new analytical and graphical methods were developed for estimation of A_w, B_s and b (feed channel friction parameter) using the experimental readings taken on spiral wound RO module. Studies on estimation of these parameters are reported in Section 4.1.

Mass transfer coefficient k is the model parameter that characterizes the concentration polarization in membrane transport. The value of k is generally estimated using standard mass transfer correlations [22,23]. Although many investigators [14,15,24] have justified the application of standard mass transfer correlations for estimation of k in membrane transport, there are a few [11,25] who have strongly criticized their validity in concentration polarization layers of membrane stating that the mechanism of solute transport in these layers is more due to advection than due to convection. Assuming the validity of mass transfer correlations of the standard form, Murthy and Gupta [20,24] have proposed a graphical method for estimation of k. However, correlations of different forms [10,11,26] have also been reported in the literature taking the effects of solvent flux, pressure and solute concentration on mass transfer coefficient. In the present work, a new correlation for estimation of k is proposed accounting for the influence of solvent flux and solute concentration in addition to fluid velocity and the validity of this correlation is justified from the experimental data.

2. Experimental studies

2.1. Experimental setup

A commercial thin film composite polyamide RO membrane packed in a spiral wound module (Make: Ion Exchange, India) was used for the experimental studies. Detailed specifications of the membrane module are given in Table 1. The schematic diagram of the experimental setup used in this work is shown in Fig. 1. The feed solution kept in a stainless steel feed tank (FT) was pumped through the spiral wound RO module (M) by a high pressure pump (P) capable of developing pressure up to 20 atm. The permeate and retentate solutions flowing out of the membrane module were collected in separate permeate (PT) and retentate (RT) collection tanks. A manual needle valve (V3) provided at the retentate outlet line was adjusted to set the fluid feed pressure. V1 and V2 are isolation valves for the high pressure pump. V4, V5 and V6 are drain valves for feed, retentate and permeate tanks respectively. Bourdon pressure gauges (PG_1 and PG_2) were installed in the feed and retentate lines to measure the inlet and outlet pressures across the membrane module. Neglecting the pressure drop on the permeate side of the membrane, the pressure on the permeate side was taken as 1 atm. Permeate and retentate flow rates were measured by means of rotameters F2 and F3 and the sum of these two flow rates was taken as the feed flow rate. The high pressure pump was provided with a variable frequency drive to adjust the speed of the motor and vary the feed flow rate between 7.5 LPM and 16 LPM. A HPLC (Perkin Elmer, USA make) unit equipped with a UV detector and C-18 column was used for the analysis and measurement of solute (chlorophenol) concentrations in retentate and permeate solutions.

2.2. Experimental methods

Aqueous feed solution of chlorophenol of specific concentration was prepared by dissolving required quantity of chlorophenol in water. Taking around 350 l of feed solution in the feed tank (FT), the RO unit was operated at a fixed inlet pressure and a fixed feed flow

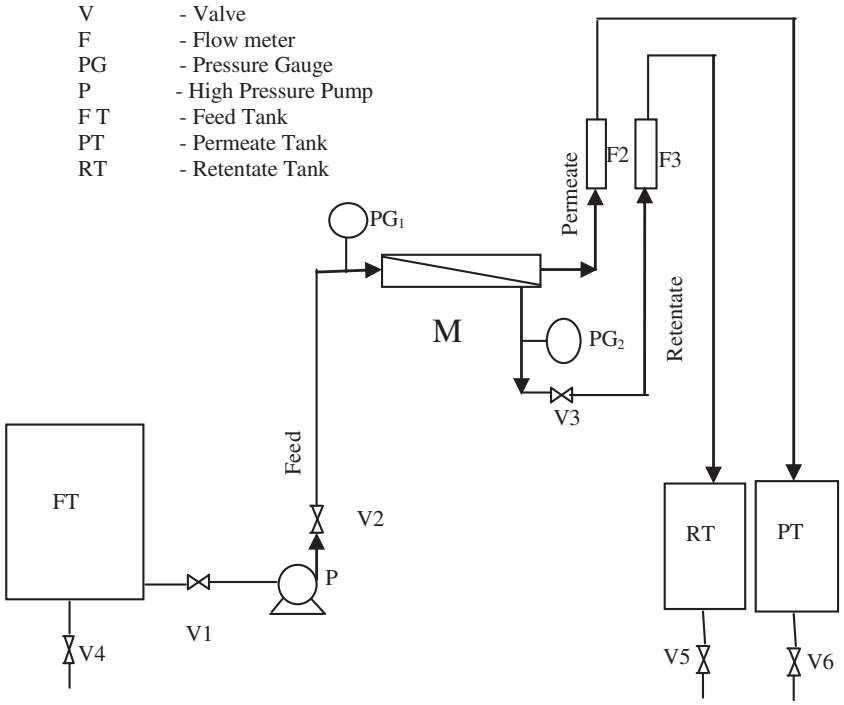

Fig. 1. Schematic diagram of the experimental set up.

Table 2
Experimental and theoretical data on removal of chlorophenol in the spiral wound RO module at a feed flow rate of $F_i = 2.166 \times 10^{-4}$ m^3/s.

Sr. no.	Pi (atm)	Po (atm)	T (°C)	$C_i \times 10^{+03}$ (kmol/m^3)	$F_o \times 10^{+04}$, (m^3/s)		% error	$C_p \times 10^{+03}$, (kmol/m^3)		% error	R		% error
					(Expt)	(Theo)		(Expt)	(Theo)		(Expt)	(Theo)	
1	5.83	4.53	30.0	0.778	1.800	1.885	−4.709	0.370	0.363	1.811	0.567	0.567	−0.032
2	7.77	6.43	30.0	0.778	1.670	1.748	−4.667	0.368	0.369	−0.050	0.593	0.579	2.315
3	9.71	8.30	30.0	0.778	1.590	1.613	−1.416	0.366	0.381	−4.135	0.614	0.583	5.083
4	11.64	10.08	30.0	0.778	1.500	1.479	1.382	0.363	0.397	−9.568	0.638	0.584	8.443
5	13.58	12.04	30.0	0.778	1.370	1.347	1.687	0.360	0.416	−15.446	0.662	0.584	11.821
6	5.83	4.48	32.0	1.556	1.851	1.902	−2.741	0.652	0.610	6.390	0.619	0.639	−3.164
7	7.77	6.38	32.0	1.556	1.736	1.772	−2.070	0.642	0.602	6.188	0.639	0.659	−3.168
8	9.71	8.25	32.0	1.556	1.630	1.644	−0.849	0.631	0.612	3.014	0.659	0.670	−1.661
9	11.64	10.13	32.0	1.556	1.523	1.518	0.308	0.624	0.630	−0.970	0.679	0.677	0.266
10	13.58	12.00	32.0	1.556	1.416	1.394	1.539	0.615	0.654	−6.357	0.700	0.682	2.642
11	5.83	4.44	32.0	2.335	1.868	1.915	−2.518	0.886	0.828	6.501	0.656	0.673	−2.544
12	7.77	6.33	32.0	2.335	1.761	1.790	−1.662	0.884	0.803	9.135	0.668	0.698	−4.390
13	9.71	8.20	32.0	2.335	1.666	1.667	−0.075	0.882	0.806	8.636	0.684	0.711	−4.064
14	11.64	10.08	32.0	2.335	1.566	1.547	1.219	0.880	0.822	6.645	0.696	0.721	−3.489
15	13.58	11.95	32.0	2.335	1.478	1.428	3.371	0.880	0.846	3.830	0.711	0.728	−2.398
16	5.83	4.39	32.0	3.891	1.898	1.936	−2.017	1.244	1.230	1.142	0.707	0.708	−0.081
17	7.77	6.28	32.0	3.891	1.808	1.819	−0.610	1.231	1.161	5.656	0.723	0.737	−1.973
18	9.71	8.15	32.0	3.891	1.681	1.703	−1.332	1.299	1.144	11.962	0.717	0.753	−5.147
19	11.64	10.03	32.0	3.891	1.650	1.590	3.615	1.198	1.149	4.071	0.748	0.765	−2.228
20	13.58	11.90	32.0	3.891	1.536	1.479	3.710	1.187	1.169	1.553	0.764	0.773	−1.289
21	5.83	4.34	31.0	6.226	1.923	1.961	−1.955	1.668	1.798	−7.768	0.755	0.731	3.143
22	7.77	6.24	31.0	6.226	1.828	1.852	−1.289	1.657	1.651	0.389	0.767	0.764	0.293
23	9.71	8.11	31.0	6.226	1.750	1.744	0.361	1.491	1.593	−6.866	0.798	0.783	1.866
24	11.64	9.98	31.0	6.226	1.641	1.638	0.176	1.475	1.577	−6.890	0.810	0.796	1.694
25	13.58	11.85	31.0	6.226	1.575	1.534	2.594	1.457	1.583	−8.619	0.819	0.806	1.609

rate. For each run, before collecting the samples for analysis, the unit was operated for about 40 min to ensure the attainment of steady state. Steady state readings of inlet pressure, outlet pressure, permeate flow rate and retentate flow rate were recorded. Permeate and retentate concentrations were measured by collecting the samples of permeate and retentate solutions and analyzing them using HPLC. The feed temperature was recorded by reading the thermometer kept in the feed tank.

For each experimental run, the steady state readings of permeate flow rate (F_p), retentate flow rate (F_o), retentate pressure (P_o), retentate concentration (C_o), permeate concentration (C_p) and feed temperature (T) were recorded for a set of fixed values of feed concentration (C_i), feed flow rate (F_i) and feed pressure (P_i). Experiments were conducted at three different feed flow rates (13, 14 and 15.5 LPM), five feed concentrations (100,200,300,500 and 800 ppm) and five feed pressures (5.83, 7.77, 9.71, 11.64 and 13.58 atm). A total of 73 readings were collected in these experimental runs and reported in Tables 2, 3 and 4. The values of Rejection coefficient R calculated using the experimental readings of C_p and C_o are also given in these tables.

$$R = 1 - \frac{C_P}{C_O} \tag{1}$$

Table 3
Experimental and theoretical data on removal of chlorophenol in the spiral wound RO module at a feed flow rate of $F_i = 2.330 \times 10^{-4}$ m^3/s.

Sr. no.	Pi (atm)	Po (atm)	T (°C)	$C_i \times 10^{+03}$ (kmol/m^3)	$F_o \times 10^{+04}$, (m^3/s)		% error	$C_p \times 10^{+03}$, (kmol/m^3)		% error	R		% error
					(Expt)	(Theo)		(Expt)	(Theo)		(Expt)	(Theo)	
1	5.83	4.46	30.0	0.778	1.957	2.053	−4.898	0.375	0.356	5.059	0.562	0.573	−1.978
2	7.77	6.35	30.0	0.778	1.860	1.916	−2.986	0.373	0.359	3.712	0.581	0.586	−0.861
3	9.71	8.22	30.0	0.778	1.742	1.78	−2.155	0.372	0.370	0.457	0.603	0.591	2.008
4	11.64	10.09	30.0	0.778	1.639	1.646	−0.404	0.370	0.385	−3.920	0.624	0.592	5.197
5	13.58	11.96	30.0	0.778	1.542	1.513	1.916	0.367	0.401	−9.203	0.645	0.591	8.330
6	5.83	4.41	32.0	1.556	2.010	2.069	−2.952	0.632	0.598	5.319	0.629	0.643	−2.260
7	7.77	6.30	32.0	1.556	1.894	1.939	−2.366	0.625	0.587	6.001	0.646	0.665	−2.858
8	9.71	8.17	32.0	1.556	1.794	1.81	−0.884	0.618	0.594	3.861	0.664	0.676	−1.752
9	11.64	10.05	32.0	1.556	1.684	1.683	0.039	0.605	0.609	−0.800	0.686	0.683	0.495
10	13.58	11.91	32.0	1.556	1.594	1.558	2.255	0.599	0.630	−5.236	0.704	0.687	2.317
11	5.83	4.36	31.0	2.335	2.022	2.082	−2.974	0.804	0.813	−1.134	0.687	0.677	1.538
12	7.77	6.25	31.0	2.335	1.907	1.956	−2.593	0.802	0.783	2.273	0.700	0.702	−0.293
13	9.71	8.12	31.0	2.335	1.815	1.832	−0.956	0.796	0.782	1.667	0.714	0.716	−0.349
14	11.64	10.00	31.0	2.335	1.707	1.711	−0.220	0.786	0.795	−1.070	0.729	0.725	0.482
15	13.58	11.86	31.0	2.335	1.607	1.591	1.022	0.777	0.815	−4.876	0.744	0.732	1.588
16	5.83	4.32	32.5	3.891	2.072	2.103	−1.505	1.206	1.210	−0.314	0.715	0.711	0.593
17	7.77	6.21	32.5	3.891	1.974	1.985	−0.555	1.213	1.134	6.522	0.724	0.741	−2.240
18	9.71	8.07	32.5	3.891	1.887	1.868	0.998	1.226	1.111	9.378	0.732	0.757	−3.506
19	11.64	9.95	32.5	3.891	1.805	1.754	2.836	1.248	1.112	10.897	0.734	0.769	−4.710
20	13.58	11.82	32.5	3.891	1.722	1.641	4.708	1.286	1.127	12.392	0.737	0.777	−5.477
21	5.83	4.27	31.0	6.226	2.082	2.127	−2.161	1.726	1.772	−2.663	0.745	0.734	1.514
22	7.77	6.16	31.0	6.226	1.987	2.017	−1.500	1.645	1.614	1.883	0.766	0.768	−0.161
23	9.71	8.03	31.0	6.226	1.902	1.908	−0.295	1.472	1.550	−5.314	0.798	0.787	1.480
24	11.64	9.90	31.0	6.226	1.815	1.801	0.795	1.433	1.528	−6.615	0.812	0.799	1.609
25	13.58	11.77	31.0	6.226	1.734	1.695	2.255	1.419	1.527	−7.692	0.822	0.809	1.632

Table 4
Experimental and theoretical data on removal of chlorophenol in the spiral wound RO module at a feed flow rate of $F_i = 2.583 \times 10^{-4}$ m^3/s.

Sr. no.	Pi (atm)	Po (atm)	T (°C)	$C_i \times 10^{+03}$ (kmol/m^3)	$F_o \times 10^{+04}$, (m^3/s)		% error	$C_p \times 10^{+03}$, (kmol/m^3)		% error	R		% error
					(Expt)	(Theo)		(Expt)	(Theo)		(Expt)	(Theo)	
1	5.83	4.34	29.5	0.778	2.200	2.312	−5.103	0.359	0.347	3.363	0.578	0.582	−0.565
2	7.77	6.22	29.5	0.778	2.075	2.174	−4.785	0.352	0.347	1.611	0.606	0.596	1.562
3	9.71	8.09	29.5	0.778	1.953	2.038	−4.326	0.347	0.355	−2.481	0.628	0.601	4.317
4	11.64	9.97	29.5	0.778	1.838	1.903	−3.517	0.343	0.368	−7.192	0.643	0.603	6.353
5	13.58	11.84	29.5	0.778	1.720	1.768	−2.815	0.34	0.382	−12.311	0.663	0.602	9.109
6	5.83	4.29	31.0	1.556	2.262	2.328	−2.917	0.591	0.583	1.402	0.652	0.649	0.436
7	7.77	6.17	31.0	1.556	2.148	2.196	−2.254	0.572	0.567	0.988	0.675	0.672	0.375
8	9.71	7.79	31.0	1.556	2.042	2.066	−1.189	0.553	0.57	−3.023	0.697	0.684	1.824
9	11.64	9.92	31.0	1.556	1.947	1.938	0.443	0.55	0.582	−5.713	0.712	0.691	2.992
10	13.58	11.79	31.0	1.556	1.850	1.812	2.082	0.549	0.598	−9.051	0.725	0.695	4.071
11	5.83	4.24	31.0	2.335	2.290	2.340	−2.203	0.767	0.794	−3.548	0.699	0.682	2.548
12	7.77	6.13	31.0	2.335	2.173	2.214	−1.868	0.752	0.757	−0.600	0.717	0.709	1.119
13	9.71	8.03	31.0	2.335	2.080	2.088	−0.392	0.744	0.751	−0.970	0.728	0.723	0.622
14	11.64	9.84	31.0	2.335	1.970	1.965	0.254	0.733	0.758	−3.463	0.742	0.732	1.370
15	13.58	11.74	31.0	2.335	1.868	1.843	1.338	0.726	0.774	−7.143	0.757	0.739	2.456
16	9.71	7.95	32.0	3.891	2.113	2.123	−0.457	1.126	1.068	5.157	0.750	0.763	−1.654
17	11.64	9.80	32.0	3.891	2.070	2.006	3.071	1.108	1.063	4.065	0.761	0.774	−1.717
18	13.58	11.69	32.0	3.891	1.972	1.891	4.087	1.092	1.072	1.858	0.774	0.782	−1.127
19	5.83	4.15	31.0	6.226	2.337	2.384	−2.014	1.845	1.741	5.624	0.726	0.736	−1.429
20	7.77	6.03	31.0	6.226	2.253	2.272	−0.857	1.549	1.566	−1.121	0.778	0.772	0.758
21	9.71	7.90	31.0	6.226	2.170	2.161	0.399	1.486	1.493	−0.491	0.794	0.791	0.316
22	11.64	9.75	31.0	6.226	2.090	2.052	1.805	1.387	1.463	−5.507	0.815	0.804	1.398
23	13.58	11.65	31.0	6.226	2.012	1.944	3.364	1.325	1.457	−9.933	0.830	0.813	2.002

3. Model equations

The experimental data reported here was used for the analysis and validation of the mathematical model developed in this work for spiral wound RO modules. The model equations, presented in Part I of this paper series[1], were solved to yield analytical expressions for the prediction of retentate flow rate (F_o), retentate pressure (P_o), retentate concentration (C_o), permeate concentration (C_p) and solvent flux (J_v). The model has four parameters namely solvent transport coefficient A_w, solute transport coefficient B_s, feed channel friction parameter b and mass transfer coefficient k. A summary of essential model equations required for model validation is presented in this section.

The equations for flow rate F(x), solvent flux $J_v(x)$, pressure $P_b(x)$ and solute concentration $C_b(x)$ in the feed channel at a distance x from the feed inlet are listed below

$$F(x) = \frac{F_o \sinh\frac{\varnothing x}{L} + F_i \sinh\varnothing\left(1-\frac{x}{L}\right)}{\sinh\varnothing} \tag{2}$$

$$J_V(x) = \frac{\varnothing}{A_m \sinh\varnothing}\left[F_i \cosh\varnothing\left(1-\frac{x}{L}\right) - F_o \cosh\frac{\varnothing x}{L}\right] \tag{3}$$

$$P_b(x) = P_i - \frac{bL}{\varnothing\sinh\varnothing}\left[F_o\left(\cosh\frac{\varnothing x}{L}-1\right) - F_i\left(\cosh\varnothing\left(1-\frac{x}{L}\right) - \cosh\varnothing\right)\right] \tag{4}$$

$$C_b(x) = C_p + \frac{F_i(C_i - C_p)}{F(x)} \tag{5}$$

where, ∅ is the dimensionless parameter defined as

$$\varnothing = L\sqrt{\frac{WbA_w}{\left(1 + A_w\left(\frac{Y}{B_s}\right)TC_p\right)}}. \tag{6}$$

L is the length of the module, W is the width of the flat membrane rolled and packed into the module and γ is the gas law constant. The solute flux $J_v(x)$ evaluated at x = 0 and x = L are

$$J_v(0) = \frac{A_W \cdot \Delta P_i}{1 + \left(\frac{A_W \gamma}{B_s}\right)TC_p} \tag{7}$$

$$J_v(L) = \frac{A_W \cdot \Delta P_o}{1 + \left(\frac{A_W \gamma}{B_s}\right)TC_p} \tag{8}$$

where ΔP_i and ΔP_o are the transmembrane pressures at x = 0 and x = L respectively

$$\Delta P_i = P_i - P_p \tag{9}$$

$$\Delta P_o = P_o - P_p. \tag{10}$$

The equations for retentate flow F_o, retentate pressure P_o and retentate concentration C_o are

$$F_o = F_i \cosh\varnothing - \frac{\varnothing\sinh\varnothing}{bL}\Delta P_i \tag{11}$$

$$P_o = P_i - \frac{bL}{\varnothing\sinh\varnothing}[(F_i + F_o)(\cosh\varnothing - 1)] \tag{12}$$

$$C_o = C_p + \frac{F_i(C_i - C_p)}{Fo}. \tag{13}$$

The equations for permeate concentration C_p evaluated at x = 0 and x = L are

$$C_p = \frac{C_i}{\left[1 + \frac{J_v(0)/B_s}{e^{Jv(0)/ki}}\right]} \tag{14}$$

$$C_p = \frac{C_o}{\left[1 + \frac{J_v(L)/B_s}{e^{J_V(L)/k_0}}\right]} \tag{15}$$

where k_i and k_o are the mass transfer coefficients at feed channel inlet and outlet respectively.

4. Estimation of model parameters

Parameter estimation for the analytical model developed in this work is an important aspect of this study. Analytical and graphical methods for parameter estimation were developed and reported in Part I of this paper series [1]. Applying these parameter estimation techniques, the values of model parameters A_w, B_s, b and k were calculated using the experimental readings reported in Tables 2, 3 and 4. The results of this parameter estimation study are outlined in this section.

4.1. Estimation of A_w, B_s and b

The dimensionless parameter ∅ was calculated for each one of the readings reported in Tables 2, 3 and 4, taking the measured values of F_i, F_o, P_i and P_o using the equation given below

$$\varnothing = cosh^{-1}\left[\frac{(F_i + F_0) - \beta \cdot F_o}{(F_i + F_0) - \beta \cdot F_i}\right] \tag{16}$$

where β is the ratio of pressure drop (P_i–P_O) on the feed channel side to the transmembrane pressure (P_I–P_P) at the feed inlet

$$\beta = \frac{P_i - P_o}{P_i - P_p}. \tag{17}$$

It is inferred from Eq. (12) that a plot of (P_i–P_o) vs $\frac{L}{\varnothing sinh \varnothing}[(F_i + F_o)(cosh\varnothing - 1)]$ will be a straight line passing through origin with slope equal to b. The parameter b is estimated by making a straight line fit of data points marked on this plot and evaluating the slope of the line so obtained. For the experimental data reported in this work, the value of b was estimated as 8529.45 $\frac{atm \cdot s}{m^4}$.

Rewriting the Eq. (6) for ∅ as below

$$\frac{1}{\varnothing^2} = \left(\frac{\gamma}{L^2 W b B_s}\right) T C_p + \left(\frac{1}{L^2 W b A_w}\right) \tag{18}$$

we obtain an expression from which it is evident that a plot of $\frac{1}{\varnothing^2}$ vs T C_p is a straight line with slope S_1 and intercept I_1

$$S_1 = \frac{\gamma}{L^2 W b B_s} \tag{19}$$

$$I_1 = \frac{1}{L^2 W b A_w}. \tag{20}$$

This linear plot shown in Fig. 2 was drawn using the experimental data reported in Tables 2, 3 and 4. The slope S_1 and intercept I_1 of the best linear fit were evaluated by the method of least squares and values of model parameters A_w and B_s were estimated using Eqs. (19) and (20). The estimated values of model parameters are $A_w = 9.5188 \times 10^{-7}$ and $B_s = 8.468 \times 10^{-8}$. The experimental data points were observed to fit the straight line with regression coefficient R^2 equal to 0.89. The values of estimated model parameters are given in Table 5.

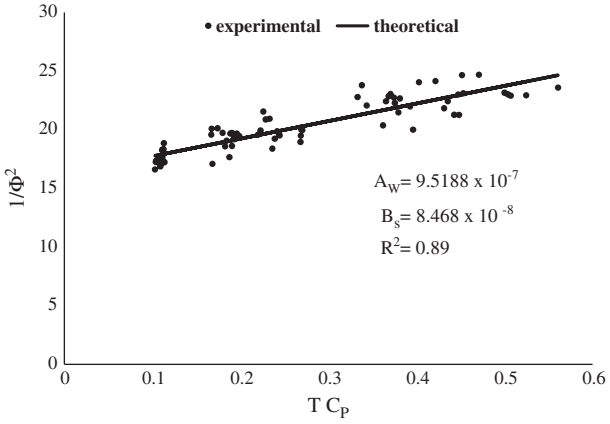

Fig. 2. Plot of $\frac{1}{\varnothing^2}$ vs T C_p for estimation of A_w and B_s.

4.2. Estimation of mass transfer coefficient k

In order to establish the influence of various factors affecting mass transfer coefficient, the value of k was assumed to vary from one end to the other end of the feed channel with varying conditions of pressure, flow rate, and solute concentration. So, for each one of the experimental readings reported in Tables 2, 3 and 4, two values of mass transfer coefficients, one at feed inlet and the other at feed outlet, were estimated using the equations given belowat feed inlet (x = 0),

$$k = \frac{J_V(0)}{ln\left[\frac{J_V(0)}{B_s}\left(\frac{C_p}{C_i - C_p}\right)\right]} \tag{21}$$

at feed outlet (x = L),

$$k = \frac{J_V(L)}{ln\left[\frac{J_V(L)}{B_s}\left(\frac{C_p}{C_0 - C_p}\right)\right]}. \tag{22}$$

In the preceding equations, the values of solute flux $J_v(0)$ and $J_v(L)$ were calculated using Eqs. (7) and (8).

So, for a set of 73 experimental readings reported in this study, a total of 146 values of k were calculated. An analysis of variation of k with respect to other variables showed that k was influenced not only by fluid velocity but also by other factors like solvent flux and solute concentration. This was in confirmation with the results reported by other investigators [11,26,27]. So it was evident from these experiments that, for the system studied in this work, the mass transfer in concentration polarization layer was influenced more severely by 'advection' than by 'convection'. Hence, the conventional correlations [22,23] reported for estimation of mass transfer coefficient which are applicable for convective transport are not valid here.

From the analysis of mass transfer coefficient values estimated using the experimental data, it is proposed that the influence of

Table 5
Value of model parameters A_W, B_S and b.

Parameter	Value
b $\frac{atm \cdot s}{m^4}$	8529.45
A_W $\frac{m}{atm \cdot s}$	9.5188×10^{-7}
B_S $\frac{m}{s}$	8.468×10^{-8}

solvent flux J_v, solute concentration C_b and fluid velocity v_f on mass transfer coefficient k may be represented by a correlation of the form

$$Sh = a\, Re_p^{n1} C_m^{n2} Re_f^{n3} \tag{23}$$

where the dimensionless numbers appearing in this correlation are defined as follows

$$Sh = \text{Sherwood number} = \frac{k\, d_e}{D_A} \tag{24}$$

$$Re_P = \text{Permeate Reynolds number} = \frac{\rho d_e J_v}{\mu} \tag{25}$$

$$C_m = \text{Dimensionless solute concentration} = \frac{C_b}{\rho_m} \tag{26}$$

$$Re_f = \text{Fluid Reynolds Number} = \frac{\rho\, d_e v_f}{\mu}. \tag{27}$$

Here d_e is the equivalent diameter of the rectangular feed channel of thickness t_f

$$d_e = 2\, t_f \tag{28}$$

and ρ_m is the molal density of water (55.56 kmol/m^3). The Permeate Reynolds number Re_p in Eq. (25) was defined to account for the influence of solvent flux J_v on k. The coefficient a and the exponents n1, n2 and n3 in Eq. (23) were estimated by the method of least square using the experimental readings given in Tables 2, 3 and 4. The correlation for Sherwood number Sh obtained from the experimental data is

$$Sh = 147.4\, Re_p^{0.739} C_m^{0.135} Re_f^{0.130}. \tag{29}$$

Fig. 3 shows a linear fit of the experimental data with the correlation (29). The regression coefficient R^2 of the fit is 0.99. The correlation shows that the permeate Reynolds number, Re_p has a much stronger influence on mass transfer coefficient than the fluid Reynolds number, Re_f. Generally, for laminar flow (Re_f<2100), the exponent of fluid Reynolds number Re_f assumes a value of 0.33 in standard correlations [23,24] reported for mass transfer coefficients. In comparison to this value, the exponent of Re_f in the proposed correlation (Eq. (29)) is much lower.

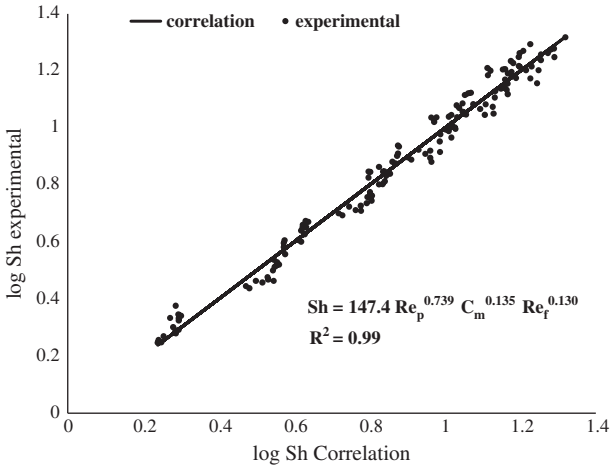

Fig. 3. Linear fit of experimental data with mass transfer correlation.

The effect of solute properties on mass transfer coefficient k can be accounted for by introducing the Schmidt number Sc $\left(Sc = \frac{\mu}{\rho D_A}\right)$ term in correlation (23) and rewriting it in the form

$$Sh = a^1 Sc^{n0} Re_p^{n1} C_m^{n2} Re_f^{n3}. \tag{30}$$

However, a large number of experiments similar to the ones reported in this study need to be performed with a number of chemical compounds to evaluate the coefficients a^1 and n0 in Eq. (30).

5. Model predictions and experimental verification

Any mathematical model gets accepted as an appropriate analytical tool only if the model predictions match with the experimental measurements within some acceptable magnitude of error. Studies carried out in this work on validation of mathematical model with experimental data are presented in this section.

For specified values of feed pressure P_i, feed flow rate F_i, feed concentration C_i, permeate pressure P_p and feed temperature T, the model developed in this work can predict the values of retentate pressure P_o, retentate flow F_o, retentate concentration C_o, permeate concentration C_p and rejection coefficient R. The estimated values of model parameters A_w, B_s and b given in Table 5 are used in these calculations. The mass transfer correlation (Eq. (29)) developed in this work is used for estimation of k.

The iterative calculation steps (algorithm) for model predictions are outlined here.

- Step 1: Assume permeate concentration $C_p = C_{pa}$ (Initial guess for $C_{pa} = 0.5{*}C_i$)
- Step 2: Calculate ∅ using Eq. (6)
- Step 3: Calculate ΔP_i using Eq. (9)
- Step 4: Calculate F_o using Eq. (11)
- Step 5: Calculate P_o using Eq. (12)
- Step 6: Calculate ΔP_o using Eq. (10)
- Step 7: Calculate $J_v(0)$ and $J_v(L)$ using Eqs. (7) and (8)
- Step 8: Calculate the fluid velocities $v_{fi} = F_i/A_f$ and $v_{fo} = F_o/A_f$ (A_f is feed channel area)
- Step 9: Calculate C_o using Eq. (13)
- Step 10: Calculate Re_p, C_m and Re_f using Eqs. (25), (26) and (27) at inlet and outlet
- Step 11: Calculate k at inlet (k_i) and outlet (k_o) using the correlation (29)
- Step 12: Calculate C_p at inlet (C_{pi}) and at outlet (C_{po}) using Eqs. (14) and (15)
- Step 13: Calculate $C_p = 0.5{*}(C_{pi} + C_{po})$
- Step 14: Compare calculated C_p (step 13) with assumed C_p ($= C_{pa}$) On convergence of calculated C_p to assumed C_p, Go to Step 16 else Go to Step 15
- Step 15: Assume new value of C_{pa} as $C_{pa} = 0.5(C_p + C_{pa})$ and Go to Step 1
- Step 16: Calculate $F_p = F_i - F_o$
- Step 17: Calculate R using Eq. (1)

A computer program was developed in MATLAB language to execute this algorithm. Using this calculation procedure for each one of the readings in Tables 2, 3 and 4, the model predictions were obtained for retentate flow F_o, retentate pressure P_o, retentate concentration C_o, permeate concentration C_p and rejection coefficient R. The predicted values of F_o, C_p and R along with the experimental readings are listed in Tables 2, 3 and 4. Comparing the model predictions with the experimental observations, it is evident that the model is able to predict the values of retentate flow F_o within 4% error for 90% of the readings, permeate concentration C_p within 10% error for 93% of the readings and rejection coefficient R within 5% error for 90% of the readings. Comparisons of theoretical model predictions

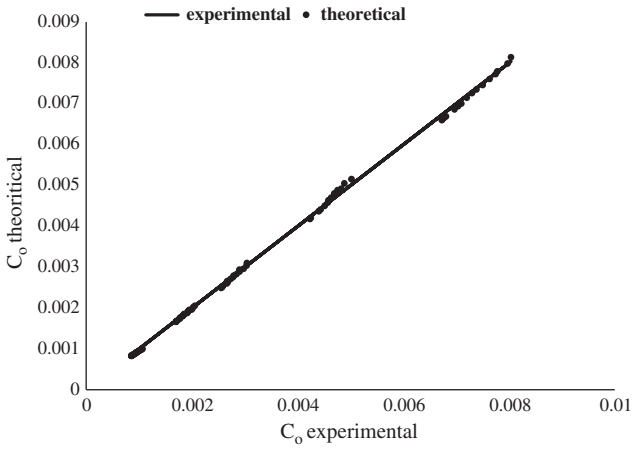

Fig. 4. Comparison of theoretical and experimental values of C_o.

with experimental readings of retentate concentration C_o and retentate pressure P_o shown in Figs. 4 and 5 respectively demonstrate a good agreement. These results demonstrate that the analytical model developed in this work has good predictive capability under various operating conditions.

6. Conclusions

An analytical model for predicting the performance of spiral wound RO modules was developed and presented in part I of this paper series[1] assuming spatial variations of pressure, flow and solute concentration in feed channel and uniform condition of pressure in permeate channel. In this paper, which is Part II of this series, experimental studies on validation and analysis of this mathematical model were presented. Experiments were conducted on a laboratory scale spiral wound RO module taking chloropenol as a model solute. A total of 73 experimental readings were collected and reported in this work by conducting experiments in which feed flow rate, feed concentration and feed pressure were varied and the readings of retentate flow rate, retentate concentration, retentate pressure and permeate concentration were recorded.

New analytical and graphical methods were developed for estimation of four model parameters namely solvent transport coefficient A_w, solute transport coefficient B_s, feed channel friction parameter b and the mass transfer coefficient k. These parameters were estimated using the experimental data reported in this work. An analysis of the estimated values of k showed that the mass transfer coefficient k was influenced not only by fluid velocity but also by solvent flux and solute concentration. Taking the influence of solvent flux J_v, solute concentration c and fluid velocity v_f on mass transfer coefficient k, a new correlation for estimation of mass transfer coefficient was proposed in this work. This correlation suggested that it was the mechanism of 'advection' more than 'convection' that influenced the mass transfer in concentration polarization layer of the membrane module.

Using the estimated values of parameters A_w, B_s, b and k in the model equations, the predictive capability of the model in validating the experimental data was tested. The results suggested that the analytical model developed in this work was capable of predicting the performance of spiral wound RO module within 4% error for retentate flow F_o, 10% error for permeate concentration C_p and 5% error for rejection coefficient R.

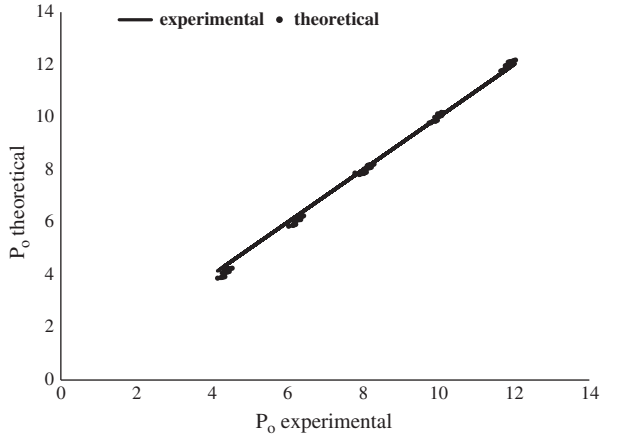

Fig. 5. Comparison of theoretical and experimental values of P_o.

Symbols

a	Coefficient appearing in Eq. (23)
a^1	Coefficient appearing in Eq. (30)
A_f	Feed channel area (m^2)
A_m	Membrane area (m^2)
A_p	Permeate channel area (m^2)
A_w	Solvent transport coefficient (m/atm·s)
b	Feed channel friction parameter (atm·s/m^4)
B_s	Solute transport coefficient(m/s)
C	Solute concentration in feed channel(kmol/m^3)
C_b	Bulk solute concentration in the feed channel (kmol/m^3)
C_i	Concentration of solute in the feed (kmol/m^3)
C_o	Concentration of solute in the retentate (kmol/m^3)
C_p	Concentration of solute in the permeate (kmol/m^3)
C_{pa}	Assumed value of C_p in the iterative calculation steps (kmol/m^3)
C_{pi}	value of C_p at module inlet (kmol/m^3)
C_{po}	value of C_p at module outlet (kmol/m^3)
C_m	Dimensionless solute concentration in Eq. (26)
C_w	Concentration of solute at the membrane wall (kmol/m^3)
d_e	Equivalent diameter of feed channel (m)
D	Module diameter (m)
D_A	Diffusivity (m^2/s)
F_i	Feed flow rate (m^3/s)
F_p	Permeate flow rate (m^3/s)
F_o	Retentate flow rate (m^3/s)
J_S	Solute flux (kmol of solute/m^2 s)
J_V	Solvent flux (m/s)
K	Mass transfer coefficient (m/s)
k_i	Mass transfer coefficient at the inlet (m/s)
k_o	Mass transfer coefficient at the outlet (m/s)
L	RO module length (m)
n	Number of turns in the spiral wound module
P_b	Pressure in the feed channel (atm)
P_i	Pressure at the feed inlet (atm)
P_o	Pressure at the feed channel outlet (atm)
P_p	Pressure in the permeate channel (atm)
n0	Exponent of Schmidt number appearing in Eq. (30)
n1	Exponent of permeate Reynolds number appearing in Eqs. (23) and (30)
n2	Exponent of dimensionless solute concentration appearing in Eqs. (23) and (30)
n3	Exponent of fluid Reynolds number appearing in Eqs. (23) and (30)
R	Rejection coefficient
Re_p	Permeate Reynolds number in Eq. (25)
Re_f	Fluid Reynolds number in Eq. (27)
Sh	Sherwood Number in Eq. (24)
Sc	Schmidt Number in Eq. (30)
t_f	Feed spacer thickness, mm

t_P	Permeate channel thickness, mm
T	Temperature (K)
v_f	Fluid velocity in feed channel (m/s)
v_{fi}	Fluid velocity at channel inlet (m/s)
v_{fo}	Fluid velocity at channel outlet (m/s)
W	RO module width (m)
x	Axial position in feed channel

Greek symbols

β	A dimensionless parameter, defined in Eq. (17)
Δ	Difference across the membrane
$\emptyset$	Dimensionless term defined in Eq. (6)
γ	Gas law constant $\left(\gamma = R, 0.0820 \frac{atm\,m^3}{^oK\,kmol}\right)$
μ	Viscosity (kg/ms)
Π	Osmotic pressure (atm)
ρ	fluid density (kg/m^3)
ρ_m	molal density of water (55.56 kmol/m^3)

References

[1] S. Sundaramoorthy, G. Srinivasan and D.V.R. Murthy, 'An analytical model for spiral wound reverse osmosis membrane modules : Part-1-Model development and Parameter estimation', Desalination (in press), doi:10.1016/j.desal.2011.03.047.

[2] S. Loeb, S. Sourirajan, Sea water demineralization by means of an osmotic membrane, Adv. Chem. Ser. 38 (1962) 117.

[3] W. Guo, R. Zhang, S. Vigneswaran, H. Ngo, J.K. Kandasamy, Membranes coupled with physico chemical treatment in water reuse, Water Sci. Technol. 61 (2010) 513–519.

[4] T. Nguyen, S. Vigneswaran, H. Ngo, H. Shon, J.K. Kandasamy, Arsenic removal by a membrane hybrid filtration system, Desalination 236 (2009) 363–369.

[5] F.C. Schutte, The rejection of specific organic compounds by reverse osmosis membranes, Desalination 158 (2003) 285–294.

[6] K. Kimura, G. Amy, J.E. Drewes, T. Heberer, T. Kim, Y. Watanabe, Rejection of organic micropollutants (disinfection by-products, endocrine disrupting compounds and pharmaceutically active compounds) by NF/RO membranes, J. Membr. Sci. 227 (2003) 113–121.

[7] A. Allegrezza, Commercial reverse osmosis membranes and modules, in: B. Parekh (Ed.), Reverse Osmosis Technology, Marcel Dekker, Inc., New York, 1988, pp. 53–120.

[8] F. Evangelista, A short cut method for the design of reverse osmosis desalination plants, Ind. Eng. Chem. Process Des. Dev. 24 (1985) 211–223.

[9] M.N.A. Hawlader, J.C. Ho, A. Malek, An experimental and analytical study of permasep-b10 separation characteristics, J. Membr. Sci. 87 (1994) 1–21.

[10] S. Avlonitis, W.T. Hanbury, M. Ben Boudinar, Spiral wound modules performance. An analytical solution: part I, Desalination 81 (1991) 191–208.

[11] S. Avlonitis, W.T. Hanbury, M. Ben Boudinar, Spiral wound modules performance. An analytical solution: part II, Desalination 89 (1993) 227–246.

[12] S.K. Gupta, Analytical design equations for reverse osmosis systems, Ind. Eng. Chem. Process Des. Dev. 24 (1985) 1240.

[13] K.K. Sirkar, P.T. Dong, G.H. Rao, Approximate design equations for reverse osmosis desalination by spiral wound modules, Chem. Eng Sci 21 (1982) 517–527.

[14] M. Ben Boudinar, W.T. Hanbury, S. Avlonitis, Numerical simulation and optimisation of spiral-wound modules, Desalination 86 (1992) 273–290.

[15] S. Senthilmurugan, Aruj Ahluwalia, S.K. Gupta, Modeling of a spiral-wound module and estimation of model parameters using numerical techniques, Desalination 173 (2005) 269–286.

[16] F. Evangelista, G. Jonsson, Optimum design and performance of spiral wound modules I: numerical method, Chem. Engn. Comm. 72 (1988) 69–81.

[17] H. Lonsdale, E.A. Mason, Statistical–mechanical theory of membrane transport, J. Membr. Sci. 51 (1990) 1–81.

[18] Y. Taniguchi, An analysis of reverse osmosis characteristics of ROGA spiral-wound modules, Desalination 25 (1978) 71.

[19] Z.V.P. Murthy, S.K. Gupta, Sodium cyanide separation and parameter estimation for reverse osmosis thin film composite polyamide membrane, J. Membr. Sci. 154 (1999) 89–103.

[20] Z.V.P. Murthy, S.K. Gupta, Simple graphical method to estimate membrane transport parameters and mass transfer coefficient in a membrane cell, Sep. Sci. Technol. 31 (1996) 77–94.

[21] D. Bhattacharyya, M.R. Madadi, Separation of phenolic compounds by low pressure composite membranes: mathematical model and experimental results, AIChE Symp. Ser. 84 (261) (1988) 139.

[22] P.C. Wankat, Rate-Controlled Separations, Springer International, 1994.

[23] G. Schock, A. Miquel, Mass transfer and pressure loss in spiral wound modules, Desalination 64 (1987) 339–352.

[24] Z.V.P. Murthy, S.K. Gupta, Estimation of mass transfer coefficient using a combined nonlinear membrane transport and film theory model, Desalination 109 (1997) 39–49.

[25] G. Belfort, N. Negata, Fluid mechanics and cross-filtration filtration: some thoughts, Desalination 53 (1985) 57.

[26] P. Erikson, Water and salt transport through two types of polyamide composite membranes, J. Membr. Sci 36 (1988) 297–313.

[27] V. Geraldes, V. Semilao, M.N. Pinho, Flow and mass transfer modelling of nanofiltration, J. Membr. Sci. 191 (2001) 109–128.